

## A Modified Two Dimensional Volterra-Based Series for the Low-Pass Equivalent Behavioral Modeling of RF Power Amplifiers

Elton J. Bonfim and Eduardo G. de Lima\*

**Abstract**—This work proposes a modified Volterra-based series suitable for the low-pass equivalent behavioral modeling of radio frequency power amplifiers (RFPAs) for wireless communication systems. In a Volterra-based series, the instantaneous sample of the complex-valued output envelope is calculated by the sum of products that depend on the instantaneous and past (up to the memory length  $M$ ) samples of the complex-valued input envelope. To comply with the constraints imposed by the bandpass behavior of RFPAs, the derivation of the proposed model starts from a general Volterra-based series given by the sum of contributions that include exactly one complex-valued information multiplied by a varying number (ranging from zero up to one less than the polynomial order truncation  $P$ ) of real-valued amplitude components. A first reduction in the number of parameters is then performed by retaining only the one and two dimensional contributions. A second reduction in the number of parameters is finally achieved by introducing a third truncation factor  $S$ . In fact, if this additional truncation factor  $S$  is set equal to  $P-1$ , the proposed model contains all the two dimensional contributions. Moreover, when  $S$  is set equal to 0, the proposed model reduces to the largely adopted generalized memory polynomial (GMP) model. The proposed Volterra-based series retains the important property of being linear in its parameters and, in comparison with previous Volterra-based approaches, can provide a better compromise between number of parameters and modeling error. The proposed model is then compared with the GMP model in a scenario of same number of parameters. When applied to the modeling of input-output data obtained from a circuit-level description of a GaN HEMT Doherty PA excited by a LTE OFDMA signal, the proposed model reduces the normalized mean square error (NMSE) by up to 3.4 dB. Additionally, when applied to the modeling of input-output data measured on a GaN HEMT class AB PA excited by a WCDMA signal, the proposed model reduces the NMSE by up to 1.3 dB.

### 1. INTRODUCTION

The improvement of power efficiency in modern wireless communication systems has received a lot of attention from the microwave community [1, 2]. Indeed, in mobile units higher efficiency is motivated by the desire of extending the time interval between two consecutive battery recharges. Besides, in base stations, economical indicators are the main drivers for power efficiency enhancement, once lower efficiency significantly increases the energy consumption and also demands for costly heat dissipation systems. Notwithstanding, the increasing number of novel wireless applications together with very fast growing number of new users of such services drastically raises the total amount of energy dealt with in wireless systems. As a consequence, green information technology politics further appoints toward the necessity of a reduction in the energy demanded by such systems [3].

Achieving high efficiency is very challenging in nowadays wireless communication systems by two reasons. First, to provide extremely high data rates with good quality of service, wireless communication standards strongly rely on the linear processing of the information signal throughout the transmitter

---

*Received 28 December 2015, Accepted 15 March 2016, Scheduled 20 March 2016*

\* Corresponding author: Eduardo Goncalves de Lima (elima@eletrica.ufpr.br).

The authors are with the Department of Electrical Engineering, Federal University of Paraná, Centro Politécnico, CP. 19011, Curitiba, PR 81531-980, Brazil.

chain. In fact, due to the limited available bandwidth for wireless systems, the adopted strategy for attaining higher data rates is to vary, according to the information signal, both the amplitude and phase of a radio frequency (RF) carrier signal [4]. However, if an amplitude modulated RF carrier signal is subject to the action of a nonlinear operator, the signal bandwidth is broadened, in this way causing the interference among users allocated into adjacent channels. Second, the most power consuming equipment in a wireless system, which is the power amplifier (PA) placed in the transmitter chain just before the antenna, cannot deliver high efficiency when operating in linear regimes or, conversely, can only guarantee high efficiency if driven at nonlinear regimes [5].

To exploit the PA operation at its highest power efficiency, the generated nonlinear distortions must be somehow cancelled out. An effective way for doing that is to purposely distort the complex-valued envelope signal before its application to the PA, by choosing a model for this so-called digital predistorter (DPD) that behaves in an inverse manner with respect to the PA [6]. In this context, a model for the PA based on measurements taking at its input and output, without any knowledge about its specific circuit, is required. Indeed, the effectiveness of a DPD is mainly dictated by the selection of an accurate and low-complexity PA behavioral model [7].

The dynamic nonlinear transfer characteristic, relating complex-valued envelope signals at the PA input and output, can be modeled by Volterra-based series [8]. In one hand, being linear in the parameters is the major advantage of Volterra-based series, because the model identification can be easily performed using standard linear techniques, such as the least squares algorithm [8]. On the other hand, the extremely high computational complexity, or equivalently the huge number of parameters, is the main drawback of Volterra-based series, once accurate models may require larger values for the polynomial order and memory length truncations. In literature, different strategies for reducing the number of parameters of Volterra-based series, at the cost of a slight deterioration in modeling accuracy, have been proposed [9–13]. Among those strategies, the generalized memory polynomial (GMP) model of [13] is up to date one of the most common choice. The GMP model can be seen as a particular instance of a Volterra-based series where only a subset of two dimensional contributions are retained.

The contribution of this work is to present a modified Volterra-based series that, in comparison with the previous approaches, can show an improved trade-off between modeling fidelity and modeling simplicity. The strategy followed here to prune a general Volterra-based series is based on the combination of two approaches: retaining only the two dimensional contributions and introducing an additional truncation factor  $S$  that can assume any integer value from zero up to one less than the polynomial order truncation  $P$ . In fact, the number of parameters of the proposed model increases with  $S$ . In particular, the maximum number of parameters is obtained when  $S$  is set equal to  $P - 1$ , in a situation where the proposed model contains all the possible two dimensional contributions. As the value of  $S$  is reduced, some of the two dimensional contributions are neglected by the proposed model. Indeed, when  $S$  is set to its minimum value, e.g., equal to 0, the proposed model reduces to the GMP model of [13].

The organization of this work is as the following. Section 2 describes the main aspects of RFPA low-pass equivalent behavioral modeling. Section 3 contains the theoretical development of the proposed Volterra-based series. Section 4 reports two case studies to illustrate the superior performance of the proposed model in comparison with the GMP model of same computational complexity. Conclusions are detailed in Section 5.

## 2. POWER AMPLIFIER LOW-PASS EQUIVALENT BEHAVIORAL MODELING

In wireless communication systems, the input signal applied to the PA is given by:

$$x(t) = \Re[\tilde{x}(t) \exp(j\omega_c t)] = a(t) \cos(\omega_c t + \theta(t)), \quad (1)$$

where  $\omega_c$  is the carrier frequency and  $\tilde{x}$  the complex-valued envelope signal whose real-valued amplitude and angle components, in a polar representation, are designated by  $a$  and  $\theta$ , respectively. The input signal of Eq. (1) has a bandwidth much lower than its center frequency, and consequently, its energy is concentrated exclusively near  $\omega_c$ . When the bandpass signal of Eq. (1) is processed through nonlinearities found in the PA internal circuit, significant power levels are generated at frequencies not excited by Eq. (1). Indeed, nonlinear distortions are responsible for the generation of considerable amounts of energy at frequencies in the vicinity of  $\omega_c$ , as well as at harmonic frequencies of  $\omega_c$ . However,

only intermodulation distortions near  $\omega_c$  are measurable at the PA output, because PA circuits are equipped with frequency-selective output matching networks that ideally remove all the spectral content located at harmonic frequencies of  $\omega_c$ . In this scenario, the signal measured at the PA output is given by:

$$y(t) = \Re [\tilde{y}(t) \exp(j\omega_c t)] = b(t) \cos (\omega_c t + \varphi(t) + \theta(t)), \quad (2)$$

where  $\tilde{y}$  is the complex-valued envelope signal whose real-valued amplitude, and angle components, in a polar representation, are designated by  $b$  and  $\varphi + \theta$ , respectively.

Non-recursive PA behavioral models, which predict the PA output signal based solely on the input signal and without knowledge of the PA internal circuit, are the preferable models for linearization purposes due to their reduced computational complexity. Apart from dealing with nonlinearities, an accurate PA behavioral model must also be able to work with dynamic effects. Indeed, while nonlinearities are associated to gain compression and saturation mechanisms that take place at the power transistor, dynamic effects occur due to non-ideal frequency responses of passive circuits, either in low-frequency range (for instance, the bias circuit) or in high-frequency range (specially input and output matching networks). Discrete-time models can represent memory effects by assuming that the instantaneous sample of the output signal is not only affected by the applied input at that same time instant, but also conditioned by the input values applied at past time instants. In fact, any input applied at a particular time instance does somehow affect the output at present and all future time instants. However, such an effect decreases as the time interval between the applied input and measured output is increased. Because of this fading memory property of PAs, negligible degradation in modeling accuracy is verified if the output is restricted to be a function of the present plus a finite number of previous input samples.

In a behavioral model that relates the bandpass output signal  $y$  as a function of the bandpass input signal  $x$ , the sampling frequency must be set equal to a few harmonics of the carrier frequency  $\omega_c$ . In this case, when the time-domain data estimated by the model are converted into frequency-domain, the base-band, fundamental and lower-order harmonic zones are clearly identified. However, a tremendous reduction in the sampling frequency can be achieved if different frequency zones (base-band, fundamental and harmonics) are allowed to overlap at frequencies around zero. To do that, first remove the negative contents of the fundamental and harmonic zones and then shift in frequency the positive spectral contents of the fundamental and harmonic zones, in a way that all zones are centered around zero. This is equivalent to having a mathematical description for the PA behavioral model that relates complex-valued input and output envelope signals [14]. In these low-pass equivalent models, a value equal to some harmonics of the envelope bandwidth can be adopted for the sampling frequency. In this way, in low-pass equivalent models, the exact frequency location of a specific contribution cannot be judged by a simple observation of the frequency spectrum [14]. Therefore, care must be taken in order to avoid the generation, by the low-pass equivalent model, of contributions located at harmonic frequencies of  $\omega_c$ , which cannot be measured in physical PAs, and hence, such contributions will increase the number of calculations required to provide the estimations without any improvement in the accuracies of the estimations [14].

### 3. THEORETICAL DEVELOPMENT

Volterra-based series have been widely adopted for the low-pass equivalent behavioral modeling of RFPAs [9–13]. A discrete-time Volterra-based series can model dynamic effects because the instantaneous sample of the complex-valued output envelope  $\tilde{y}(n)$  is dependent on the instantaneous ( $n$ ) and past ( $n - m$ ) samples of the complex-valued input envelope, where  $m$  is a positive integer number ranging from 0 up to the memory length  $M$ . A Volterra-based series can estimate nonlinear mechanisms because the complex-valued output envelope is a polynomial function of the complex-valued input envelope. In other words, a Volterra-based series has first-order terms in which the output is proportional to the input, second-order terms in which the output is proportional to the product of two inputs, third-order terms in which the output is given by the product of three inputs, and so on until terms of infinite dimension. In practice, the polynomial order must be truncated by a polynomial

order  $P$ . The constitutive equation of a general Volterra-based series is given by:

$$\tilde{y}(n) = \sum_{p=0}^{P-1} \sum_{m_1=0}^M \sum_{m_2=0}^M \sum_{m_3=0}^M \dots \sum_{m_{p+1}=m_p}^M \tilde{h}_{p+1,m_1,m_2,\dots,m_{p+1}} \tilde{x}(n-m_1) \prod_{j=1}^p |\tilde{x}(n-m_{j+1})| \quad (3)$$

where  $\tilde{h}_{p+1,m_1,m_2,\dots,m_{p+1}}$  are the Volterra-based series complex-valued coefficients. The operator module  $|\cdot|$  extracts the amplitude component of a complex-valued number. A Volterra-based series can be seen as a sum of products (or, equivalently, contributions), where each product has its own and exclusive parameter. Therefore, a Volterra-based series is linear in its parameters, and as a consequence, its coefficients can be identified using linear techniques as the least squares algorithm [8].

In each product of Eq. (3), one and only one input envelope is kept unchanged, e.g., without the presence of the operator module  $|\cdot|$ . All the remaining input envelopes are changed by the presence of the operator module. All the contributions of Eq. (3) are indeed contributions at the fundamental zone (around  $1\omega_c$ ). The proof is as follows. First, observe that any complex-valued input represents an information at the fundamental zone (around  $1\omega_c$ ). For example, the complex-valued envelope  $\tilde{x}(n-m)$  is related to the real-valued signal  $x(n-m)$  by  $x(n-m) = |\tilde{x}(n-m)| \cos[1\omega_c(n-m) + 1\angle\tilde{x}(n-m)]$ . Second, observe that any amplitude component of a complex-valued envelope represents a contribution at the DC zone (around  $0\omega_c$ ). For example,  $a(n-m) = |\tilde{x}(n-m)| = |\tilde{x}(n-m)| \cos[0\omega_c(n-m) + 0\angle\tilde{x}(n-m)]$ . Third, observe that the exact frequency location of a contribution given by the product of input information can be determined by performing the addition of the integer numbers that multiply  $\omega_c$  in each individual input information. Such knowledge is applied twice: a) the product of two or more informations located at the DC zone always provides a contribution located at the DC zone, because the sum of several zeros is still zero — as an example,  $|\tilde{x}(n-m_1)||\tilde{x}(n-m_2)| = |\tilde{x}(n-m_1)||\tilde{x}(n-m_2)| \cos[0\omega_c(n-m_1) + 0\omega_c(n-m_2) + 0\angle\tilde{x}(n-m_1) + 0\angle\tilde{x}(n-m_2)]$ ; b) the product of one information located at the DC zone by one information located at the fundamental zone always produces a contribution located at the fundamental zone, because one plus zero is equal to one — as an example,  $|\tilde{x}(n-m_1)||\tilde{x}(n-m_2)| = |\tilde{x}(n-m_1)||\tilde{x}(n-m_2)| \cos[0\omega_c(n-m_1) + 1\omega_c(n-m_2) + 0\angle\tilde{x}(n-m_1) + 1\angle\tilde{x}(n-m_2)]$ . This concludes the proof that a general Volterra-based series described by Eq. (3) does comply with the constraints imposed by the bandpass behavior of RFPAs discussed in Section 2.

The modeling accuracy of a Volterra-based series is strongly conditioned by the truncation factors  $P$  and  $M$ . Higher accuracies are achieved for higher values of  $P$  and  $M$ . However, the number of parameters of Eq. (3) rises very rapidly with  $P$  and  $M$ . One step of the least squares algorithm consists of performing a matrix inverse. The order of the matrix to be inverted is equal to the number of parameters. When the number of parameters is very large, the matrix to be inverted tends to be ill-conditioned, e.g., almost singular, which in turn can significantly deteriorate the quality of the identified coefficients. Moreover, the computational complexity of a Volterra-based series is directly proportional to the number of parameters. Therefore, the huge number of parameters demanded for accurate predictions is a major concern in Volterra-based series. In this context, the search for strategies that can reduce the number of parameters of Volterra-based series with little effect on their modeling accuracy is highly valuable. With the purpose of reducing the number of parameters of Eq. (3), this work exploits and combines two distinct mechanisms detailed in the sequence.

A first and significant reduction in the number of parameters of Eq. (3) is possible if only the one- and two-dimensional contributions are kept. Here one-dimensional terms refer here to contributions that depend on the input applied at a single time sample, for example  $\tilde{x}(n-4)$ ,  $|\tilde{x}(n)|\tilde{x}(n)$  and  $|\tilde{x}(n-2)|^3\tilde{x}(n-2)$ . Here two-dimensional terms refer to contributions that depend on the input applied at exactly two time samples, for example  $|\tilde{x}(n-4)|\tilde{x}(n-3)$ ,  $|\tilde{x}(n)|^2\tilde{x}(n-1)$  and  $|\tilde{x}(n)|^3\tilde{x}(n-3)$ . In other words, three-dimensional terms, as  $|\tilde{x}(n-3)||\tilde{x}(n-2)|\tilde{x}(n-4)$ ,  $|\tilde{x}(n)|^2|\tilde{x}(n-4)|\tilde{x}(n-1)$  and  $|\tilde{x}(n-2)|^3|\tilde{x}(n-4)|\tilde{x}(n)$ , are neglected, as well as terms that depend on the input applied at more than three time samples. In doing that, the two-dimensional Volterra-based series is described by:

$$\tilde{y}(n) = \underbrace{\sum_{p_1=0}^{P-1} \sum_{p_2=0}^{P-1}}_{\text{if } (p_1+p_2) < P} \sum_{m_1=0}^M \sum_{m_2=0}^M \tilde{h}_{p_1,p_2,m_1,m_2} |\tilde{x}(n-m_1)|^{p_1} |\tilde{x}(n-m_2)|^{p_2} \tilde{x}(n-m_2). \quad (4)$$

To further reduce the number of parameters, Eq. (4) is modified by the introduction of an additional truncation factor  $S$  that can assume any integer value from zero up to  $P-1$ . In doing that, the modified two-dimensional Volterra-based series proposed in this work is described by:

$$\tilde{y}(n) = \underbrace{\sum_{p=0}^{P-1} \sum_{s=0}^S}_{\text{if } (s+p) < P} \sum_{m_1=0}^M \sum_{m_2=0}^M \tilde{h}_{p,s,m_1,m_2} |\tilde{x}(n-m_1)|^p |\tilde{x}(n-m_2)|^s \tilde{x}(n-m_2). \quad (5)$$

In the proposed model given by Eq. (5), the number of parameters can be changed according to  $S$ . If  $S$  is set equal to its maximum value, namely  $P-1$ , Eq. (5) includes all the two-dimensional contributions, and therefore, the resulting model is equivalent to Eq. (4). If the value of  $S$  is lower than  $P-1$ , some two-dimensional contributions are neglected by Eq. (5). Indeed, as the value of  $S$  decreases, the number of parameters of Eq. (5) also decreases. Moreover, when  $S$  is set to its minimum value, e.g., equal to 0, the proposed model reduces to:

$$\tilde{y}(n) = \sum_{p=0}^{P-1} \sum_{m_1=0}^M \sum_{m_2=0}^M \tilde{h}_{p,m_1,m_2} |\tilde{x}(n-m_1)|^p \tilde{x}(n-m_2). \quad (6)$$

The model described by Eq. (6) was previously reported in [13] and called generalized memory polynomial (GMP) model. The GMP model of Eq. (6) can be seen, therefore, as a particular instance of the modified two-dimensional Volterra-based series of Eq. (5), obtained when  $S$  is set equal to zero. Specifically, the GMP model neglects terms that contain the product of amplitude components at different time samples, for example  $|\tilde{x}(n-4)||\tilde{x}(n-3)|^3\tilde{x}(n-3)$  and  $|\tilde{x}(n-2)|^5|\tilde{x}(n-1)|^2\tilde{x}(n-1)$ . It is worth mentioning that the authors that have presented the GMP model in [13] did not provide any justification for not including the terms that contain the product of amplitude components at different time samples.

#### 4. VALIDATION

In this section, the modified two-dimensional Volterra-based series described by Eq. (5) and the GMP model given by Eq. (6) are applied to the low-pass equivalent behavioral modeling of two different devices under test (DUTs). Their modeling accuracies as a function of their respective computational complexities are then investigated. The computational complexity is estimated by the number of parameters required by the model. There are different combinations of values for  $P$ ,  $M$  and  $S$  in Eq. (5), which result in a model with the same number of parameters. Similarly, there are distinct combinations of values for  $P$  and  $M$  in Eq. (6), which result in a model with the same number of parameters. For any particular realization of Eq. (5) or (6), the number of operations demanded by the parameter extraction method is dependent on the number of parameters, but not dependent on the particular choice between Eqs. (5) and (6) and not dependent on the specific values for the truncation factors. Hence, the models described by Eqs. (5) and (6), in the case of same number of parameters, present the same computational complexity. By varying the three truncation factors of Eq. (5), namely  $M$ ,  $P$  and  $S$ , as well as the two truncation factors of Eq. (6), namely  $M$  and  $P$ , several particular realizations of Eqs. (5) and (6) having different computational complexities are achieved. Here, truncation factor  $M$  in Eqs. (5) and (6) is varied from 0 to 15, truncation factor  $P$  in Eqs. (5) and (6) varied from 0 to 45, and truncation factor  $S$  in Eq. (5) varied from 0 to  $P-1$ . The modeling accuracy is calculated by the metric normalized mean square error (NMSE), according to the definition reported in [15]. The input-output data measured on the DUTs are separated into two subsets. The subset used for the parameter identification is different from the subset employed to access the modeling accuracies. The model extraction and validation are executed in MATLAB software using double precision floating-point arithmetic. The parameter identification is performed using the least squares algorithm [8]. Using the input-output data subset for extraction, for each combination of truncation factor values, least squares algorithm is performed to identify the parameters of the modified two-dimensional Volterra-based series described by Eq. (5) and the GMP model given by Eq. (6). Using the input-output data subset for validation, the NMSE achieved by each particular instance is collected, together with the number of

parameters required by its realization. The results obtained for each DUT are reported in the following subsections.

#### 4.1. GaN HEMT Doherty Power Amplifier

The first DUT is a circuit-level description of a Doherty power amplifier, using high electron mobility transistor (HEMT) models and suitable for fabrication in GaN technology. To capture the input-output data, the DUT was excited by a carrier signal of frequency 2.14 GHz and modulated by a LTE OFDMA envelope signal having about 10 MHz of bandwidth. Figure 1 shows the NMSE results as a function of the number of parameters achieved by the proposed model of Eq. (5) and the previous GMP model of Eq. (6). Two main observations can be gathered from Figure 1. First, in a scenario of a similar number of parameters, the proposed model always shows a lower modeling error than the GMP model. Second, the lowest NMSE obtained by the GMP model is equal to  $-50.6$  dB, while the lowest NMSE obtained by the proposed model is equal to  $-54.0$  dB. Therefore, the proposed model can reduce the modeling error by up to 3.4 dB.

Another comparative analysis between the proposed model of Eq. (5) and the GMP model of Eq. (6) is illustrated in Figure 2. Figure 2 shows the power spectral densities (PSDs) of two error signals. An error signal is obtained by taking the difference between the desired output and the output estimated by the proposed model having 405 parameters. Another error signal is given by the difference between the desired output and the output estimated by the GMP model having 404 parameters. Observe that in a case of similar number of parameters, the PSD of the error signal produced by the proposed model

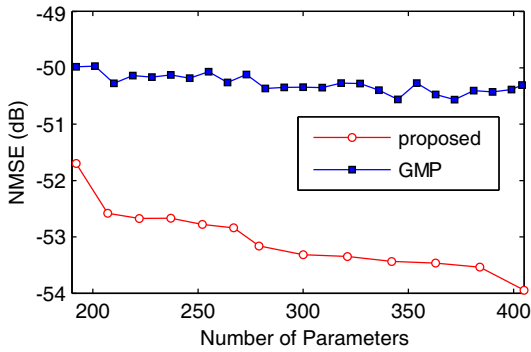


**Figure 1.** NMSE results as a function of the number of parameters.

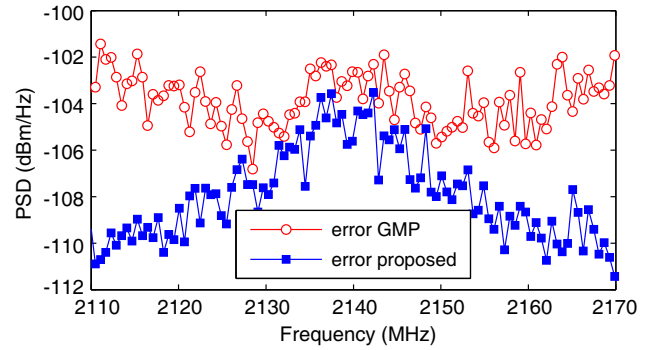


**Figure 2.** PSD of the error signals: proposed model has 405 parameters and GMP model has 404 parameters.

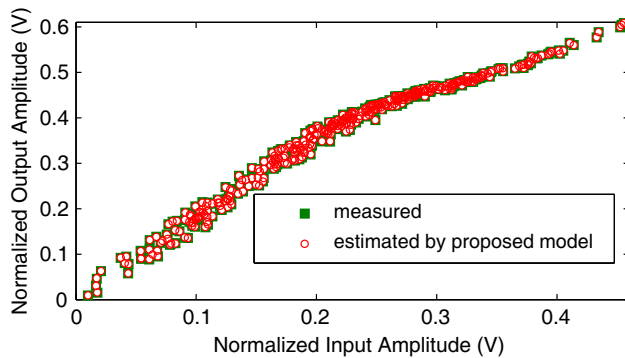


**Figure 3.** AM-AM conversions: measured and estimated by the proposed model having 405 parameters.

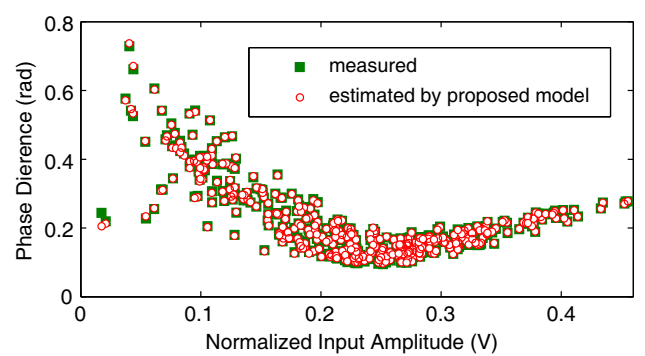


**Figure 4.** AM-PM conversions: measured and estimated by the proposed model having 405 parameters.

is significantly lower than the PSD of the error signal due to the GMP model. Moreover, the proposed model shows a superior performance in all displayed frequencies.

So far, Figures 1 and 2 have illustrated that in this case study, the proposed model of Eq. (5) can provide a better trade-off between modeling error and computational complexity than the previous GMP model of Eq. (6). At this point, attention is focused on investigating how good are the estimations provided by the proposed model. To that purpose, Figures 3 and 4 show, respectively, the measured and estimated amplitude-modulation-to-amplitude-modulation (AM-AM) and amplitude-modulation-to-phase-modulation (AM-PM) conversions. Observe that in Figures 3 and 4 there are no visible differences between measured and estimated conversions, in this way illustrating the excellent quality of the estimations provided by the proposed model.

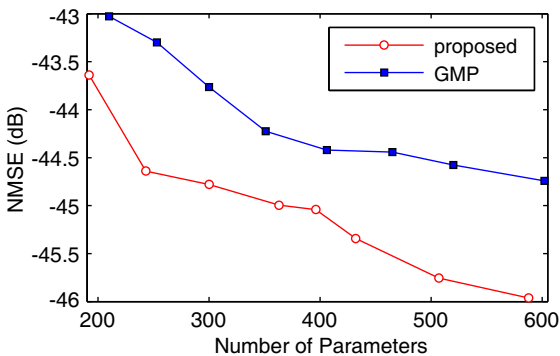
#### 4.2. GaN HEMT Class AB Power Amplifier

The second DUT is a class AB power amplifier employing a HEMT fabricated in GaN technology. The DUT was excited by a carrier signal of frequency 900 MHz and modulated by a 3GPP WCDMA envelope signal having about 3.84 MHz of bandwidth. The input-output data were measured with a Rohde & Schwarz FSQ vector signal analyzer (VSA) at a sampling frequency of 61.44 MHz.

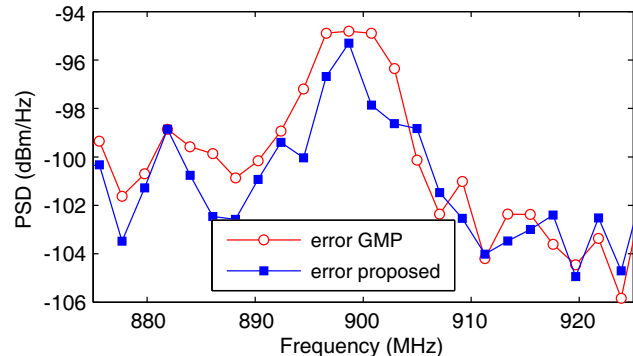
Figure 5 shows the NMSE results as a function of the number of parameters achieved by the proposed model of Eq. (5) and the previous GMP model of Eq. (6). Observe that in the case of same number of parameters, the proposed model always shows a lower modeling error than the GMP model. Specifically, the lowest NMSE obtained by the GMP model is equal to  $-44.7$  dB, while the lowest NMSE obtained by the proposed model is equal to  $-46.0$  dB. Therefore, the proposed model can reduce the modeling error by up to 1.3 dB. In fact, the GMP model needs 602 parameters to achieve its best NMSE value of  $-44.7$  dB, while the proposed model having 243 parameters can achieve a NMSE value of  $-44.6$  dB.

Figure 6 shows the PSDs of two error signals. An error signal is obtained by taking the difference between the measured output and the output estimated by the proposed model having 588 parameters. Another error signal is given by the difference between the measured output and the output estimated by the GMP model having 602 parameters. As the case with the previous DUT, the proposed model shows reduced modeling errors compared with the GMP model of similar computational complexity.

Figures 5 and 6 illustrate that once again, the proposed model of Eq. (5) can provide a better trade-off between modeling error and computational complexity than the previous GMP model of Eq. (6). The measured and estimated AM-AM and AM-PM conversions shown, respectively, in Figures 7 and 8 are included to certify the extremely high accuracy of the estimations provided by the proposed model.



**Figure 5.** NMSE results as a function of the number of parameters.



**Figure 6.** PSD of the error signals: proposed model has 588 parameters and GMP model has 602 parameters.

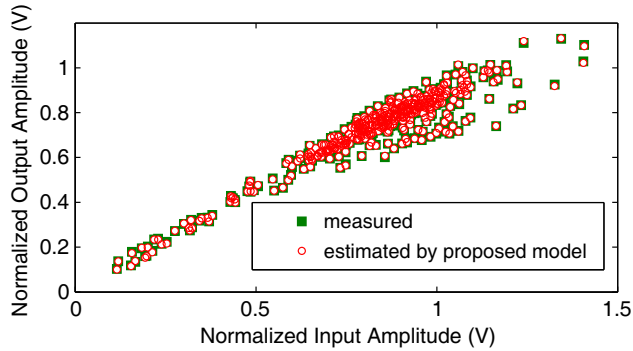


**Figure 7.** AM-AM conversions: measured and estimated by the proposed model having 588 parameters.

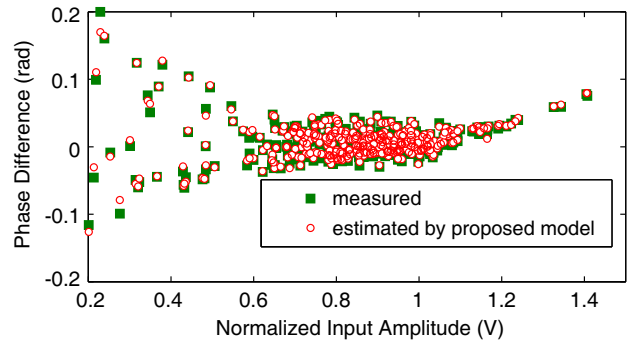


**Figure 8.** AM-PM conversions: measured and estimated by the proposed model having 588 parameters.

## 5. CONCLUSIONS

This work has addressed the behavioral modeling of RFPAs using complexity-reduced Volterra-based series. Two distinct strategies are exploited in order to derive a modified two dimensional Volterra-based model. Based on input-output data obtained from two different GaN HEMT RFPAs, the proposed model is carefully compared with the widely known generalized memory polynomial (GMP) model having a similar number of parameters. For the two studied cases, the proposed model achieves lower errors, quantified by NMSE improvements equal to 3.4 dB (for the Doherty PA) and 1.3 dB (for the class AB PA).

The major application for PA behavioral models is in the PA linearization using the digital baseband predistortion (DPD) technique. In a DPD scheme, a model with extremely high accuracy and low computational burden is of paramount importance. In one hand, the power consumption of the DPD circuitry must be kept as low as possible, once the inclusion of the linearizer is beneficial only when the power saved inside the PA is superior to the power consumed by the DPD itself. Besides, the energy dissipated by the digital hardware that implements the DPD is proportional to the number of operations required by the behavioral model. On the other hand, to increase the efficiency, especially in the presence of a linearizer, the PA is driven at high input power levels. Even in this scenario where strong nonlinear behaviors associated with power gain compression and saturation are clearly noticeable, the PA output signal must comply with very rigorous linearity metrics. For instance, the integrated output power due to the distortions at adjacent channels must be several orders of magnitude lower than the integrated output power at the main channel. In this context, any improvement in accuracy of the PA behavioral model can be significantly helpful for improving the overall efficiency. In fact, the average output power (and, more important, the efficiency) of a linearized PA can be increased until the level where the linearization metrics reach their maximum allowable values. Because the presence of nonlinearities at the output of a linearized PA is directly related to the accuracy of the behavioral model, more accurate models have the potential to allow for an increase in PA average output power, without violating any linearity requirements. Therefore, when the proposed behavioral model is applied to the PA linearization, the improvements in NMSE results offered by it (between 1.3 dB and 3.4 dB reported in this work) have the potential to considerably contribute for improving the PA efficiency, even in comparison with reference NMSE results that are already very low (on the range from  $-44$  dB to  $-51$  dB, achieved by the GMP model).

## REFERENCES

1. Ye, D., Y. Wu, and Y. Liu, "A tradeoff design of broadband power amplifier in Doherty configuration utilizing a novel coupled-line coupler," *Progress In Electromagnetics Research C*, Vol. 48, 11–19, 2014.

2. Ma, C., W. Pan, and Y.-X. Tang, "Design of asymmetrical Doherty power amplifier with reduced memory effects and enhanced back-off efficiency," *Progress In Electromagnetics Research C*, Vol. 56, 195–203, 2015.
3. Raychaudhuri, D. and N. B. Mandayam, "Frontiers of wireless and mobile communications," *Proc. IEEE*, Vol. 100, No. 4, 824–840, 2012.
4. Raab, H., P. Asbeck, S. Cripps, P. B. Kenington, Z. B. Popovic, N. Potheary, J. F. Sevic, and N. O. Sokal, "Power amplifiers and transmitters for RF and microwave," *IEEE Trans. Microw. Theory Tech.*, Vol. 50, No. 3, 814–826, 2002.
5. Cripps, S., *RF Power Amplifiers for Wireless Communications*, Artech House, Norwood, 2006.
6. Kenington, P. B., *High Linearity RF Amplifier Design*, Artech House, Norwood, 2000.
7. Chipansky Freire, L. B., C. de Franca, and E. G. de Lima, "A modified real-valued feed-forward neural network low-pass equivalent behavioral model for RF power amplifiers," *Progress In Electromagnetics Research C*, Vol. 57, 43–52, 2015.
8. Mathews, V. and G. Sicuranza, *Polynomial Signal Processing*, Wiley, New York, 2000.
9. Sun, G., C. Yu, Y. Liu, S. Li, and J. Li, "An accurate complexity-reduced simplified Volterra series for RF power amplifiers," *Progress In Electromagnetics Research C*, Vol. 47, 157–166, 2014.
10. Sun, G., C. Yu, Y. Liu, S. Li, and J. Li, "A modified generalized memory polynomial model for RF power amplifiers," *Progress In Electromagnetics Research Letters*, Vol. 47, 97–102, 2014.
11. Kim, J. and K. Konstantinou, "Digital predistortion of wideband signals based on power amplifier model with memory," *Electron. Lett.*, Vol. 37, No. 23, 1417–1418, 2001.
12. Zhu, A., J. C. Pedro, and T. J. Brazil, "Dynamic deviation reduction-based Volterra behavioral modeling of RF power amplifiers," *IEEE Trans. Microw. Theory Tech.*, Vol. 54, No. 12, 4323–4332, 2006.
13. Morgan, D., Z. Ma, J. Kim, M. Zierdt, and J. Pastalan, "A generalized memory polynomial model for digital predistortion of RF power amplifiers," *IEEE Trans. Signal Process.*, Vol. 54, No. 10, 3852–3860, 2006.
14. Lima, E. G., T. R. Cunha, and J. C. Pedro, "A physically meaningful neural network behavioral model for wireless transmitters exhibiting PM-AM/PM-PM distortions," *IEEE Trans. Microw. Theory Tech.*, Vol. 59, No. 12, 3512–3521, 2011.
15. Isaksson, M., D. Wisell, and D. Ronnow, "A comparative analysis of behavioral models for RF power amplifiers," *IEEE Trans. Microw. Theory Tech.*, Vol. 54, No. 1, 348–359, 2006.